Precambrian Research 317 (2018) 230–240

Contents lists available at ScienceDirect

Precambrian Research

journal homepage: www.elsevier.com/locate/precamres

Lead isotope constraints on the genetic relationships among different ore types in the Dongshengmiao deposit, northern China

Zhaofu Gao[a], Xiangkun Zhu[a,*], Yuan He[a], Zilong Zhou[a], Kan Zhang[a], Jian Sun[a], Jianxiong Ma[a], Zhaohua Luo[b], Chao Tang[a]

[a] MNR Key Laboratory of Isotope Geology, MNR Key Laboratory of Deep-Earth Dynamics, Institute of Geology, Chinese Academy of Geological Sciences, Beijing 100037, China

[b] School of Earth Sciences and Resources, China University of Geosciences, Beijing 100083, China

ARTICLE INFO

Keywords:
Pb isotopes
Genetic relationship
Sulfide vein
Stratiform orebody
SEDEX-type deposit

ABSTRACT

The giant Dongshengmiao Cu-Zn-Pb-S deposit is the most representative Proterozoic sedimentary exhalative (SEDEX) deposit in China. A detailed investigation of Pb isotope compositions of sulfides from various types of ores and associated host rocks has been carried out to determine the genetic relationships among different ore types and to provide important insights on whether younger fluids have contributed mineralizing materials in the formation of the Dongshengmiao Cu-Zn-Pb ores. The substantial similarity of the Pb isotope composition between the studied stratiform Cu-Zn-Pb and S orebodies suggests that the bulk of the Dongshengmiao Cu-Zn-Pb ores belong to the same polymetallic metallogenic system with the syngenetic S ores of the Proterozoic age. Comparatively, vein-type ores show relative scattered Pb isotope signatures that fall along a well-correlated linear trend, whereas their less radiogenic end member projects towards the Pb isotope compositions of the overlying stratiform main orebody. In addition, the overall Pb isotope compositions of these vein-type ores have shown an apparent overlap and similar trend with the radiogenic disseminated pyrites in the mica schists, indicating their radiogenic Pb most likely originated from host rocks as well. The scatter of Pb isotope compositions of the Dongshengmiao Cu-Zn-Pb ores shows that lead was not homogenized regionally during subsequent metamorphism, ruling out the possibility of a deposit-scale remobilization. Furthermore, the significant difference and lack of intermediate Pb isotope values between the previously studied Hercynian feldspars and the bulk of the Dongshengmiao sulfide ores suggest that a significant introduction of metals from, or overprinting by, fluids derived from Hercynian magmatism is unlikely to have played an important role in the metal endowment. Taken together, all sulfide orebodies associated with various ore types in the Dongshengmiao deposit belong to an integrated and progressive hydrothermal ore-forming system of the Proterozoic age, and a portion of the vein-type ores and associated disseminated pyrites experienced a minor addition of evolved rock lead during subsequent greenschist face metamorphisms.

1. Introduction

The Paleoproterozoic Langshan-Zhaertai basin (Zhaertai Group) of northern China hosts several strata-bound Zn-Pb deposits, which are largely hosted within a sequence of carbonaceous mica schist and marble deposited in an E-W trending marginal rift setting (Li et al., 2007). The Dongshengmiao deposit, with reserves of 4.83 million tons (Mt) of Zn at an average grade of 2.85% Zn, 0.96 Mt of Pb at 0.67% Pb and 0.11 Mt of Cu at 0.86% Cu (Long, 2009), represents the largest known Cu-Zn-Pb deposit in the Langshan-Zhaertai area. It has been exploited since the early 1970s, down to 500 m below the surface. The Dongshengmiao deposit shows many features that are characteristic of sedimentary exhalative (SEDEX) deposits, including the predominantly metasedimentary host rocks, the stratiform feature of the orebodies, the presence of layered sulfides and barites, and the highly positive sulfur isotope composition ($\delta^{34}S$: +15‰ ~ +40‰; Xia and Zhao, 1990; Ding and Jiang, 2000; Gao et al., 2015).

The giant Dongshengmiao deposit is a complex polymetallic hydrothermal deposit characterized by a wide range of styles. Previous studies have shown strong texture contrasts between the S ore and Cu-Zn-Pb ore (Xia, 1992; Zhang et al., 2010; Gao et al., 2014; Zhong et al., 2015a). Massive S ore is the most voluminous style of mineralization

* Corresponding author.
E-mail address: xiangkun@cags.ac.cn (X. Zhu).

https://doi.org/10.1016/j.precamres.2018.09.002
Received 25 October 2017; Received in revised form 1 September 2018; Accepted 11 September 2018
Available online 14 September 2018

and is widely regarded as being of syngenetic origin, whereas the metallogenic processes of the most economical Cu-Zn-Pb ore, as well as its possible genetic links to the syngenetic S ore, still remain controversial. Traditionally, the characteristic brecciated Cu-Zn-Pb ores at Dongshengmiao have been interpreted as a syngenetic proximal facies and the breccias were regarded as the result of the boiling of hydrothermal fluids (Xiu, 1987). The associated vein-type ores are considered feeders of the overlying stratiform orebodies (Jiang, 1994). In this model, sulfide ores in the Dongshengmiao deposit were slightly modified during subsequent metamorphism and deformation (Li et al., 1986; Xia, 1992; Jiang, 1994; Zhou et al., 2012). However, large-scale fluid-assisted remobilization of preexisting mineralizing materials from surrounding rocks or early-formed orebodies has been proposed to account for the Dongshengmiao Cu-Zn-Pb mineralization by some recent studies (Zhang et al., 2010; Zhong et al., 2015a; Zhong and Li, 2016). In this model, the parental sulfides have been almost totally redistributed during regional metamorphism and deformation. Remarkably, some studies have stressed that younger fluids may also contribute mineralizing materials in the formation of the Dongshengmiao Cu-Zn-Pb ores to explain an unusually great Cu endowment compared to most SEDEX-type deposits (Peng et al., 2007a,b; Zhong and Li, 2016). For example, based on the study of decrepitating temperatures of fluid inclusions, Peng et al. (2007a) proposed that Hercynian magmatic overprinting was responsible for the vein-type ores. Zhong and Li (2016) also emphasized that the abnormally enriched Cu in the Dongshengmiao deposit was derived from the source of metamorphic fluid during the early Cretaceous period based on thermodynamic modeling.

Deciphering the genetic relationships between different orebodies and ore types in a large polymetallic hydrothermal deposit is vital for establishing the deposit's metallogenesis. Pb isotope analysis for ore deposits can be a powerful tool in this respect (Mukasa et al., 1990; Velasco et al., 1996; Marcoux, 1998; Anderson et al., 2002; Ayuso et al., 2014; Potra and Macfarlane, 2014). Previous Pb isotopic studies of the Dongshengmiao deposit (Li et al., 1986; Ding and Jiang, 2000) provided valuable source and approximate age information. However, these studies focused mainly on regional characteristics concerning several deposits where the types of samples used for Pb isotope analyses were not clearly specified. Thus, the results are of limited use in determining the genetic relationships among different ore types in the same deposit. Furthermore, no Pb isotope investigation has been performed on Cu ores to date.

In this study, Pb isotope compositions of the vein-type ores and stratiform massive orebodies (S ore, Zn-Pb ore and Cu ore) from different stratigraphic positions, together with disseminated pyrites in the Dongshengmiao deposit are investigated to determine their genetic relationships. In particular, we present the first Pb isotope data of chalcopyrite samples in order to determine whether younger fluids have played an important role in the unusually great Cu endowment at Dongshengmiao.

2. Geological setting

2.1. Regional geology

The Langshan-Zhaertai polymetallic ore belt is situated in the western part of the northern margin of the Northern China Craton (NCC) and extends for approximately 600 km from west to east. Numerous deposits of variable types and sizes occur in this area, including four large or giant and more than ten medium-sized sediment-hosted Cu-Zn-Pb deposits which are suggested to be from the Mesoproterozoic age (Ding and Jiang, 2000; Zhong et al, 2015a), as well as many Cu-Au deposits which are dated to the early Permian age (Zhong et al., 2015b). This study focuses on the Dongshengmiao deposit, which is located in the southwest margin of the Langshan-Zhaertai ore belt and connected to the northeast margin of the Alxa block (Fig. 1).

The oldest rocks exposed in this area are Archean basement rocks, which consist mainly of high-grade metamorphosed basaltic and sedimentary rocks from 2.65 ~ 2.51 billion years ago (Ding and Jiang, 2000; Zhong and Li, 2016). Proterozoic strata, the Zhaertai Group, unconformably overlie the Archean basement. Sandstones of the Zhaertai Group contain detrital zircon populations from approximately 2500 million years ago (Ma), indicating that the provenance of the Zhaertai Group is Archean basement rocks (Li et al., 2007). A single zircon U-Pb dating of volcanic rocks intercalated within the Zhaertai Group gives a deposition age of ca. 1750 Ma (Li et al., 2007), which is consistent with the whole rock Sm-Nd model age of the metabasalt rocks (t_{DM} = 1767–1867 Ma; Peng and Zhai, 1997). Thus, it is believed that the Zhaertai Group is largely late Paleoproterozoic in age (Bai, 1993; Peng and Zhai, 1997; Li et al., 2007; Gong et al., 2016). The Zhaertai Group, which hosts the sulfide deposits, underwent greenschist face metamorphisms during the Shinagan orogeny in the late Mesoproterozoic period (Zhang, 2004). Recently, Zhong and Li (2016) suggested that the early Cretaceous metamorphism associated with orogeny has played an important role in the formation of ore deposits. Nearly all of the Proterozoic strata in the Langshan-Zhaertai area are unconformably overlain by Cretaceous-Quaternary terrestrial sedimentary strata (Fig. 1), which are mostly composed of red sandstone, conglomerate, and mudstone. Paleozoic sedimentary strata rarely appear in this area, except for some Carboniferous-Permian marine strata (Fig. 1).

Proterozoic magmatic rocks are volumetrically minor in the Langshan-Zhaertai area (Bao et al., 2018), while younger intrusive rocks constitute a large part of this area (Fig. 1), including Late Paleozoic biotite granite, granodiorite and intermediate intrusive rocks. The emplacement of voluminous Permian granitoids may represent the main tectonic-thermal event in the northern margin of the NCC. Recent studies have revealed that almost all of the Permian granitoids in the northwestern margin of the NCC share similar geochemical characteristics, including enrichment in large ion lithophile elements (LILEs), depletion in Nb and Ta, and high radiogenic Hf isotopic signatures (Hu et al., 2015, and references therein). Early Permian granitoids are widely exposed in the northwest of the Dongshengmiao deposit and separated from the Cretaceous red sandstone layer by a thrust fault (Fig. 1B; Hu et al., 2015; Zhong and Li, 2016). Lithological units of the volumetrically huge granitoids at Dongshengmiao mainly include quartz diorite and porphyritic granite (287 ~ 275 Ma; Hu et al., 2015). In addition, minor monzogranite (259.4 ± 3.3 Ma; Wu et al., 2013) and granodiorite (228 ± 4 Ma; Liu, 2012) have been reported near the Dongshengmiao deposit.

2.2. Geology of the Dongshengmiao deposit

The Dongshengmiao sub-basin is generally interpreted to be a local, structurally controlled graben related to the spreading of the Langshan rift in the Paleoproterozoic age (Jiang, 1993). The boundary of the Dongshengmiao deposit is controlled by regional deep faults that reactivated in an extensional environment (Fig. 1B; Peng et al., 2007a). The tectonic feature of the Dongshengmiao deposit is characterized by several northeast-trending thrust faults that generally dip northwest (Fig. 1B). Synsedimentary fault, as reflected by the thickness and facies changes, has been recorded in the Dongshengmiao deposit by early studies (Jiang, 1994; Peng and Zhai, 2004).

The ore-hosting sequence in the Dongshengmiao deposit, the Zhaertai Group, comprises both meta-sedimentary and minor meta-volcanic rocks with a total thickness greater than 1317 m (Jiang, 1993; Peng and Zhai, 2004). Based on lithology and ore-bearing features, the Zhaertai Group in the mining area is traditionally subdivided into three formations (Ding and Jiang, 2000). From the bottom up, the lowest Shujigou Formation mainly comprises quartzites and mica schists, in which Cu-bearing minerals, such as chalcopyrite, chessylite, zigueline and malachite, can be commonly observed (Jiang, 1993). The Zenglongchang Formation consists mainly of pure marbles, with phosphoric metasandstone at the bottom. The lower part of the Agulugou

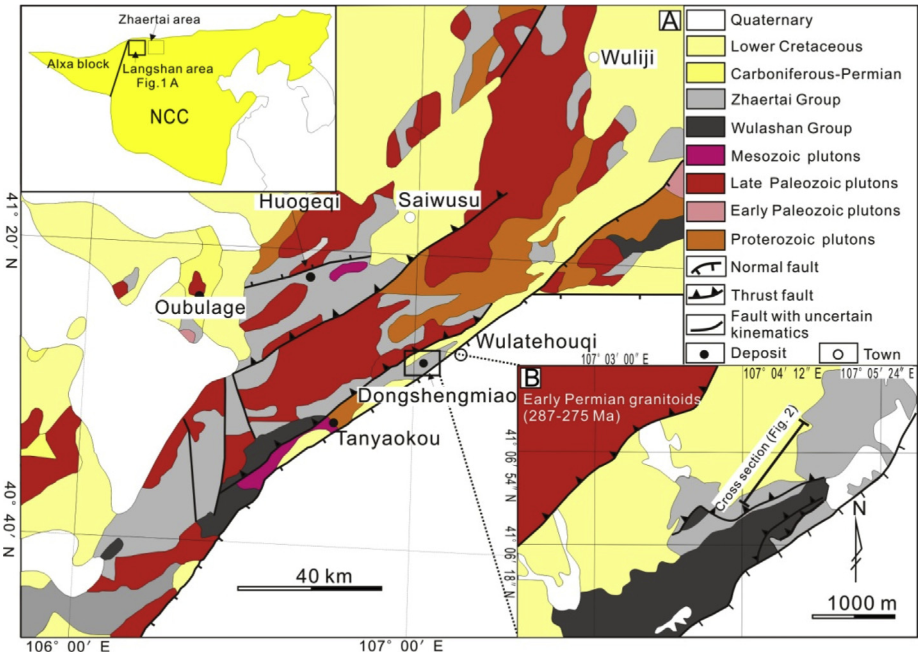

Fig. 1. A. Geological map of the Langshan area in the NCC, showing the location of the Dongshengmiao deposit in the Langshan area (modified from Peng et al., 2007b); B. Detailed geological map of the Dongshengmiao deposit (modified from Zhai et al., 2008). Early Permian granitoids are exposed in the northwest of the Dongshengmiao deposit (Hu et al., 2015).

Formation is dominated by carbonaceous mica schist with minor interbedded marble. The amount of graphite is relatively high in carbonaceous mica schists, which host extensive vein-type mineralization, as well as pervasive disseminated pyrites. In addition, meta-volcanic rocks and tuffs are intercalated mainly at the bottom of this part (Jiang, 1993; Rui et al., 1994; Peng and Zhai, 1997; Peng et al., 2007c). These alkali-enriched meta-volcanic rocks are dominated by rhyolitic to rhyodacitic meta-volcanic rocks and minor metabasalt rocks, which display bimodal features (Peng and Zhai, 1997). The upper part of the Agulugou Formation is composed of layer-shaped carbonaceous marble, which is interbedded with carbonaceous phyllite, biotite quartz schist, carbonaceous mica schist and several siderite layers.

3. Mineralization and alteration

The mineralization in the Dongshengmiao deposit took place generally parallel to sedimentary beddings at specific stratigraphic horizons (Fig. 2). Most orebodies are commonly lenticular or stratiform on a large scale, and three Cu-Zn-Pb orebodies (9# ~ 11#) locally cut across different lithological units of the host rocks. Diverse mineralization styles at Dongshengmiao were strongly controlled by lithologic units. S (predominantly pyrite) ore was mainly confined to carbonate-dominant parts of ore-bearing sequences, such as the Zenglongchang Formation and the upper part of the Agulugou Formation, whereas nearly all Pb-Zn ores and most Cu ores were hosted by carbonaceous mica schist in the lower part of the Agulugou Formation (Fig. 2).

The stratiform sulfide orebodies at Dongshengmiao can be divided into two sub-groups on the basis of their stratigraphic horizons, ore types and vertical metal zoning (Xia, 1992; Jiang, 1994). Basal stratiform mineralization includes the Cu ores in the Shujigou Formation and three adjacent S orebodies (1#, 7# and 8#) in the Zenglongchang Formation (Fig. 2). These stratiform orebodies contain minor sphalerite but no barite and siderite. By contrast, sulfide orebodies (9# ~ 11#, 2#,

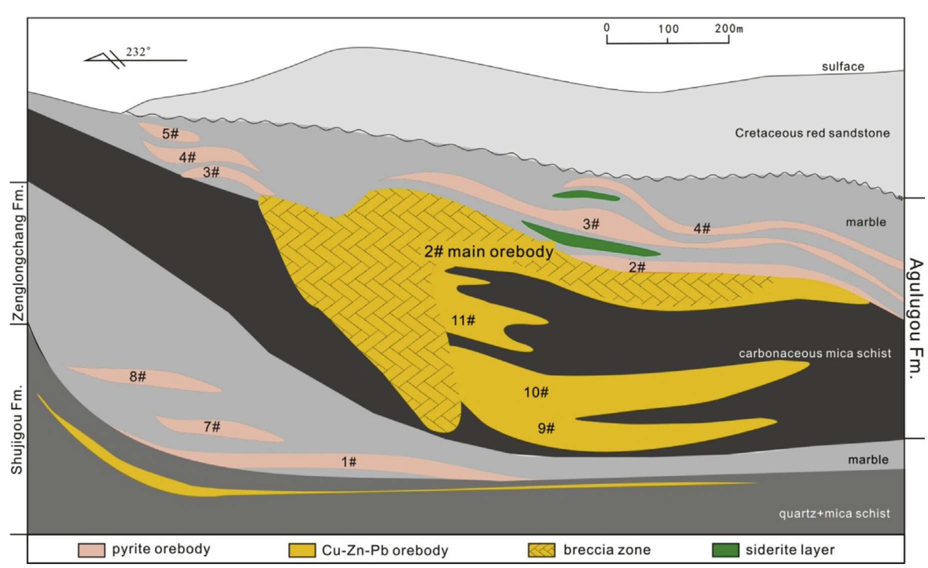

Fig. 2. Geological NE-SW cross-section modified from Peng et al. (2000), illustrating the geometry of the Dongshengmiao deposit. The section line is shown in Fig. 1B.

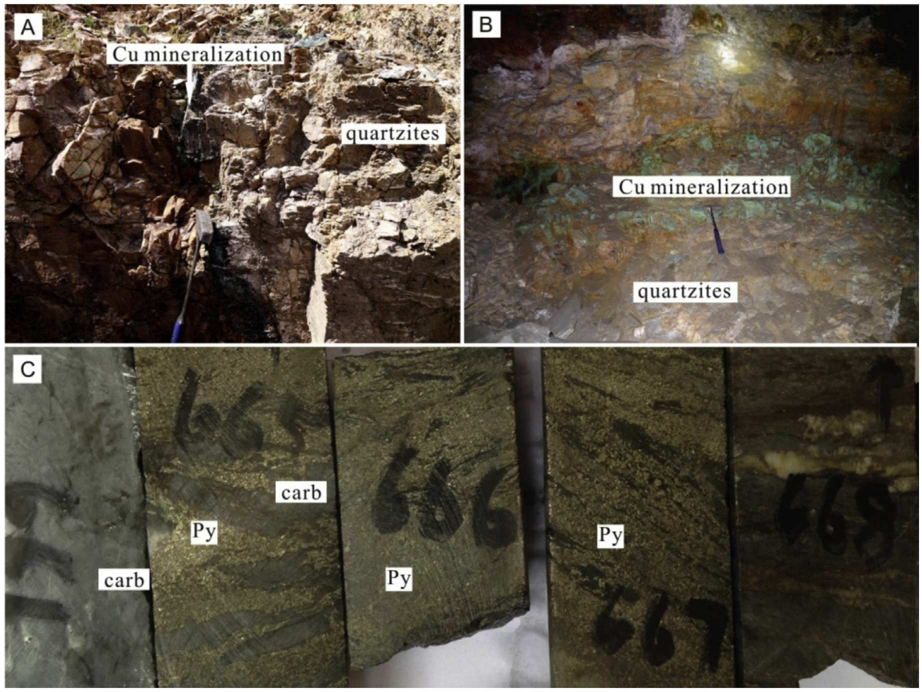

Fig. 3. Petrographic characteristics of the basal Cu-S ores in the Shujigou and Zenglongchang Formations. Abbreviations: Py = pyrite; carb = carbonate; A ~ B. Stratiform Cu orebody hosted by the basal quartzites; C. Carbonate rocks occur in the S ore (hand specimen).

and 3# ~ 5#; Fig. 2) in the Agulugou Formation contain approximately 80% of the metal reserves of the Dongshengmiao deposit. In the vertical direction, metal abundance in the several genetically related orebodies in the Agulugou Formation varies from Cu to Zn-Pb to Fe (Ba) from the bottom up, and mineral associations change from chalcopyrite + pyrrhotite + sphalerite to galena + sphalerite + pyrite to pyrite + barite + siderite.

All ore types of the Dongshengmiao deposit have been affected by variable degrees of metamorphic recrystallization and local mobilization. Most massive ores are strongly recrystallized. A portion of the Cu-Zn-Pb ores occurs in seemingly epigenetic positions relative to S ore could be resulted by local remobilization. In addition, subsequent remobilization events could be responsible for the mineralized veinlets and associated fissure mineralization hosted by carbonaceous mica schist.

3.1. Cu-S ores in the Shujigou and Zenglongchang formations

This stratiform Cu orebody in the lowest quartzites (Fig. 3A) is regarded as the early stage of the Dongshengmiao sulfide mineralization (Jiang, 1993). Cu-bearing minerals, such as chalcopyrite, chessylite, zigueline and malachite (Fig. 3B), are commonly observed in the quartzites of the Shujigou Formation. Three stratiform S orebodies occurred in the marbles of the Zenglongchang Formation. The hanging rocks and footwall rocks of these S orebodies are characterized by vein-type sulfide mineralization and intense sericitization. Silicified marble strips are commonly observed (Fig. 3C). These silicified strips have a certain orientation, roughly parallel to the sedimentary strata (Fig. 3C), which have been interpreted as dissolution-collapse breccias (Gao et al., 2014). These striped silicified rocks, which are different from irregular-shaped synsedimentary breccias, are the result of sulfide minerals partly replacing carbonate minerals.

3.2. Cu-Zn-Pb ores in the Agulugou Formation

The most economically important Cu ores (Fig. 4A, B, and C) and Zn-Pb ores (Fig. 4D, E, and F) at Dongshengmiao are mainly composed of three strata-bound orebodies (9# ~ 11#) hosted by the carbonaceous mica schist and the overlying main orebody (2#; Fig. 2). Several ore layers within a single orebody are more or less interconnected (Fig. 2; Xiu, 1987; Jiang, 1993). The main orebody (2#) occurred at the bottom of the upper carbonate-dominant part, and it is roughly conformable with the lithological boundaries (Fig. 2). This economically most important orebody has a long lateral extent (more than 1 km long) with an average thickness of ca. 15 m.

Brecciated structures are commonly observed in high grade Cu-Zn-Pb ores (Fig. 4A, D, and E), which have been interpreted as a syngenetic proximal facies, and the breccias were regarded as the result of the boiling of hydrothermal fluids (Xiu, 1987). These brecciated Cu-Zn-Pb ores from 9# ~ 11# orebodies and brecciated Zn-Pb ores from 2# orebody form a funnel-shaped breccia zone (Fig. 2) in the Dongshengmiao deposit, which may extend for more than 300 m of depth with a metal association dominated by Cu, Zn and Pb, and the ores are thought to result from multistage reactivated synsedimentary faulting (Jiang, 1993; Peng et al., 2000). These brecciated ores consist predominantly of sphalerite, pyrrhotite, galena and chalcopyrite, with a minor amount of pyrite. The angular fragments are composed of carbonaceous marble, mica schist and marble (Fig. 4). In addition, some fragments are cemented by sphalerite, pyrrhotite and galena (Fig. 4A), and sulfide-filling microfractures are well-developed within fragments (Fig. 4F). Sphalerite distributed along grain boundaries of carbonate minerals, and replaced the host carbonate (Fig. 4F). That is, the replacement of host dolomite, open space filling, and cementation of fragments derived from dissolution collapse are the common types of the Dongshengmiao brecciated Cu-Zn-Pb ores.

Vein-type sulfide ores have low grades, but they still constitute an important ore resource in the Dongshengmiao deposit. The principal ore minerals are pyrrhotite, chalcopyrite, sphalerite, galena and minor pyrite. Most minerals are anhedral, irregularly granular in shape. The chalcopyrite and pyrrhotite bearing veins are most common, however, sphalerite and galena deposited in spaced cleavages and in veins (Fig. 4G). Vein-type sulfide ores (mainly Cu ores) hosted by carbonaceous mica schist has a close association with the funnel-shaped breccia zone, making it difficult to eliminate such veins as subsurface feeders

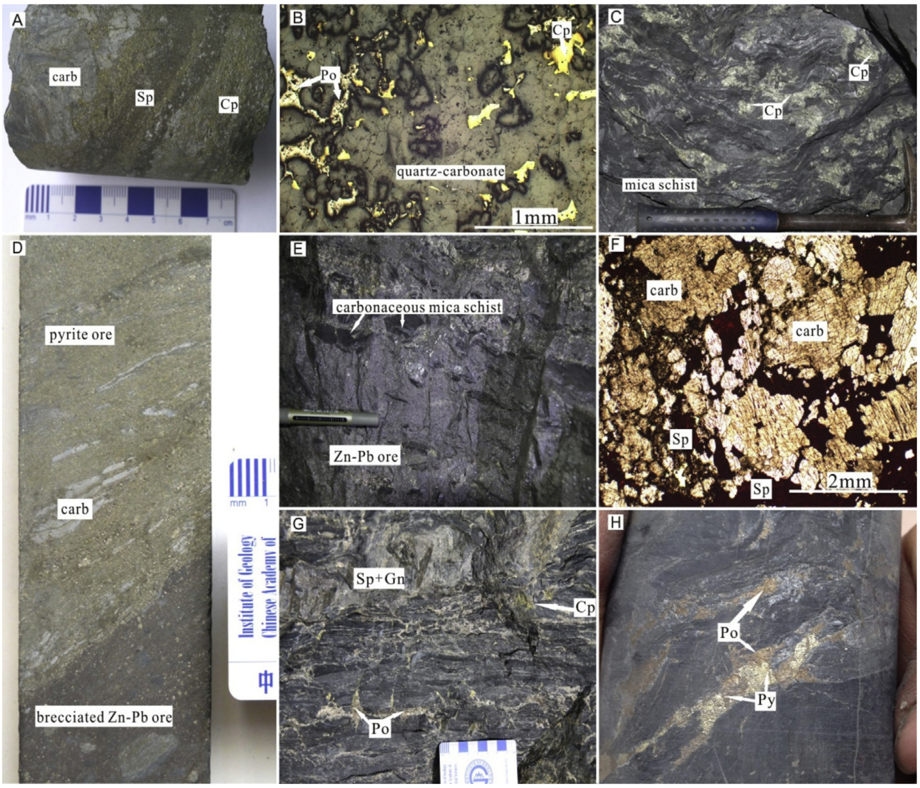

Fig. 4. Petrographic characteristics of the Cu-Zn-Pb ores in the Agulugou Formation. Abbreviations: Sp = sphalerite; Gn = galena; Po = pyrrhotite; Cp = chalcopyrite. Other abbreviations are the same as those in Fig. 3. A. Brecciated Zn-Cu ore; B. Chalcopyrite disseminated in quartz-carbonate rock; C. Chalcopyrite-pyrite veins in carbonaceous mica schist; D. Brecciated Zn-Pb ore and massive S ore; E. Brecciated Zn-Pb ore with fragments of host rocks; F. Zn-Pb ore hosted by carbonate; G. Sulfide deposited in spaced cleavages and in veins; H. Irregular-shaped pyrite was corroded and replaced by pyrrhotite, forming a residual metasomatic texture.

for the overlying stratiform orebody, which was suggested by Jiang (1993, 1994). In addition, subsequent remobilization events could be responsible for the fissure mineralization hosted by carbonaceous mica schist (Fig. 4G). Irregular-shaped disseminated pyrite was corroded and replaced by pyrrhotite, forming a residual metasomatic texture (Fig. 4H). However, based on the study of decrepitating temperatures of fluid inclusions, Peng et al. (2007a) proposed that Hercynian magmatic overprint was responsible for the vein-type ores.

3.3. S ores in the Agulugou formation

Three stratiform S orebodies occur in the upper carbonate-dominant part of the ore-bearing sequence (3# ~ 5#; Fig. 2). Siderite layers can be observed in the footwall or hanging rocks of these S orebodies (Fig. 2). These S orebodies show clear evidence of syngenetic mineralization, including stratiform morphology (Fig. 2). Massive and banded structures are predominant in these S ores, and banded S ore (Fig. 5A) is regarded as a key criterion for the recognition of syngenetic mineralization. Although a portion of massive S ores recrystallized during regional metamorphism, syngenetic fine-grained pyrites can be commonly observed. Pyrite comprises the most abundant sulfide at Dongshengmiao, and pyrrhotite is also commonly observed in these massive or banded S ores (Fig. 5A). In addition, some mineralized veinlets, mainly including pyrrhotite (Fig. 5B), sphalerite and galena, can be observed in S ore. These veinlets may be associated with the late remobilization suggested by early researchers (Li et al., 1986; Zhong and Li, 2016). Various carbonates, quartz and barite (Fig. 5C, D) are common gangue minerals. Barite is commonly peripheral to or stratigraphically above the deposit, representing a distal sedimentary facie of the Dongshengmiao deposit (Miu and Ran, 1992).

3.4. Alteration

The host rocks of the Dongshengmiao deposit show intense hydrothermal alteration, including carbonatization, silicification, sericitization, chloritization and alkali feldspathization. Silicification and sericitization are closely related to sulfide mineralization. Silicified wall rocks are commonly observed near or within S orebodies (Fig. 3C).

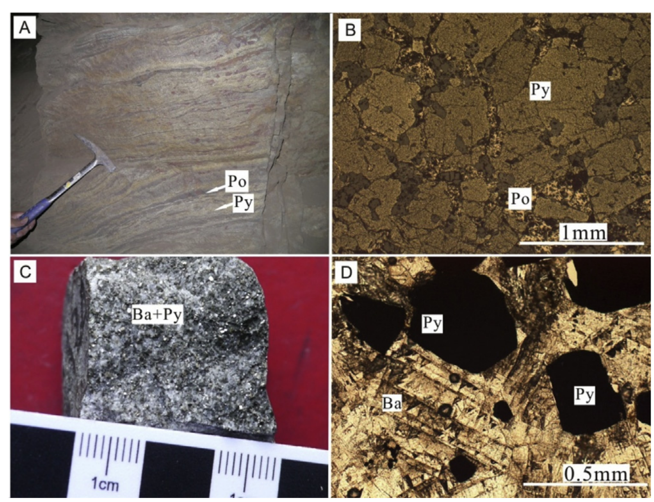

Fig. 5. Petrographic characteristics of the stratiform S ores in the Agulugou Formation. Abbreviations: Ba = barite. Other abbreviations are the same as those in Figs. 3 and 4. A. Banded S ores comprising mainly pyrite and pyrrhotite; B. Pyrrhotite veinlets in S ore; C. S-Ba ore (hand specimen); D. Barite precipitated with pyrite.

4. Materials and methods

A total of 32 samples of sulfide mineral separates were selected for Pb isotopic analysis (Table 1), including pyrite (n = 12), chalcopyrite (n = 13), pyrrhotite (n = 5) and galena (n = 2). These sulfide minerals represent the different ore types described above, including vein-type ores (n = 17) and massive S ores (n = 6) and Cu ores (n = 2) from different stratigraphic positions, together with disseminated pyrites (n = 7). Pb isotope data of brecciated Zn-Pb ores (n = 10) from the

Table 1
Pb isotope data and the U, Th, and Pb content (ppm) of sulfides from the Dongshengmiao deposit.

Sample No.	Sample	Description	$^{206}Pb/^{204}Pb$	$^{207}Pb/^{204}Pb$	$^{208}Pb/^{204}Pb$	U	Th	Pb	Model age[a] (Ma)	Reference
massive sulfide										
sulfide ore in the Agulugou Formation										
ZK3603-238	Pyrite	massive S ore, 4#	15.396	15.181	35.528	0.140	0.360	160	1775	This study
ZK3603-390A	Pyrite	brecciated Zn-Pb ore, 2#	15.166	15.150	35.326	0.430	0.190	4498	1925	Gao et al. (2018)
ZK3603-390A	Pyrrhotite	brecciated Zn-Pb ore, 2#	15.162	15.144	35.326	0.510	0.280	7550	1918	Gao et al. (2018)
WC12-3B	Galena	brecciated Zn-Pb ore, 2#	15.157	15.150	35.310				1933	Gao et al. (2018)
DSM12-2	Galena	brecciated Zn-Pb ore, 2#	15.164	15.153	35.317				1931	Gao et al. (2018)
DSM12-16	Galena	brecciated Zn-Pb ore, 2#	15.162	15.152	35.316				1932	Gao et al. (2018)
DSM12-18	Galena	brecciated Zn-Pb ore, 2#	15.154	15.148	35.300				1932	Gao et al. (2018)
WC12-1	Pyrite	brecciated Zn-Pb ore, 2#	15.170	15.149	35.326				1920	Gao et al. (2018)
WC12-3B	Pyrite	brecciated Zn-Pb ore, 2#	15.160	15.145	35.316				1922	Gao et al. (2018)
WC12-1	Sphalerite	brecciated Zn-Pb ore, 2#	15.167	15.150	35.324				1924	Gao et al. (2018)
WC12-3B	Sphalerite	brecciated Zn-Pb ore, 2#	15.158	15.145	35.314				1924	Gao et al. (2018)
ZK3603-390b	Pyrite	massive S ore, 2#	15.197	15.158	35.363	0.350	0.270	6079	1911	This study
ZK3603-380	Pyrite	massive S ore, 2#	15.202	15.151	35.356	0.060	0.200	646	1895	This study
D-8	Pyrite	massive S ore, 5#	15.202	15.144	35.281				1883	Ding and Jiang,2000
average			15.187	15.151	35.336				1909	
basal Cu-S ore										
ZK3603-667	Pyrite	massive S ore, 1#	15.107	15.109	35.112				1909	This study
ZK3607-670B	Pyrrhotite	massive S ore, 1#	14.974	15.066	34.987				1958	This study
ZK3607-670A	Pyrite	massive S ore, 1#	14.963	15.064	34.975	0.080	0.290	2241	1964	This study
D-15	Pyrite	massive S ore, 8#	15.171	15.182	35.435				1972	Ding and Jiang (2000)
990-2	Chalcopyrite	basal Cu ore	14.953	15.047	35.162	0.18	0.72	239	1944	This study
960-2	Chalcopyrite	basal Cu ore	15.159	15.109	35.137	0.1	0.12	677	1862	This study
average			15.055	15.096	35.135				1935	
vein-type ore										
13-2	Chalcopyrite	quartz-carbonate vein, 11#	15.231	15.151	35.337	< 0.05	< 0.05	17.7		This study
13-3	Chalcopyrite	quartz-carbonate vein, 11#	15.266	15.156	35.388	0.21	0.1	8.82		This study
13-20	Chalcopyrite	in mica schists, 11#	15.270	15.161	35.389					This study
13-28	Chalcopyrite	quartz-carbonate vein, 11#	15.205	15.148	35.330	< 0.05	< 0.05	148		This study
13-30	Chalcopyrite	in mica schists, 11#	15.187	15.147	35.325	0.27	0.45	1391		This study
13-32	Chalcopyrite	quartz-carbonate vein, 11#	15.531	15.198	35.659	< 0.05	< 0.05	6.98		This study
13-33	Chalcopyrite	in mica schists, 11#	15.252	15.160	35.371	0.17	0.27	2014		This study
13-35	Chalcopyrite	in mica schists, 11#	15.253	15.158	35.364	0.08	0.08	1935		This study
DSM12-111	Chalcopyrite	in mica schists	16.293	15.316	36.328					This study
DSM12-112	Chalcopyrite	in mica schists	15.713	15.203	35.709					This study
DSM12-113	Chalcopyrite	in mica schists	15.302	15.164	35.408					This study
ZK3607-370	Pyrrhotite	in mica schists	16.441	15.338	36.637					This study
ZK3607-520B	Pyrrhotite	in mica schists	16.036	15.274	36.125					This study
ZK3607-530B	Pyrrhotite	in mica schists	15.272	15.173	35.397					This study
ZK3603-380	Pyrrhotite	vein in Zn-Pb ore	15.441	15.191	35.597					This study
13-27	Galena	in mica schists, 11#	15.204	15.153	35.336					This study
ZK3603-600	Galena	in mica schists	15.237	15.168	35.369					This study
D-3	Galena	in carbonate slate	15.656	15.178	36.682					Li et al. (1986)
D-1	Sphalerite	in carbonaceous dolomite	16.301	15.320	36.194					Li et al. (1986)
D-2	Sphalerite	in marble	15.335	15.151	35.400					Li et al. (1986)
D-4	Sphalerite	in marble	15.742	15.202	35.759					Li et al. (1986)
D-5	Sphalerite	in carbonaceous slate	15.415	15.145	35.253					Li et al. (1986)
D-6	Sphalerite	in marble	15.732	15.221	35.771					Li et al. (1986)
D-7	Sphalerite	in marble	15.728	15.234	35.826					Li et al. (1986)
average			15.543	15.196	35.665					
disseminated pyrite in mica schists										
DSM12-57	Pyrite	in mica schists	15.857	15.247	35.926					This study
ZK3607-400	Pyrite	in mica schists	16.168	15.254	35.956					This study
ZK3607-490	Pyrite	in mica schists	15.316	15.169	35.439					This study
ZK3607-430	Pyrite	in mica schists	17.540	15.482	37.590					This study
ZK3607-500	Pyrite	in mica schists	15.295	15.159	35.391					This study
ZK3607-520A	Pyrite	in mica schists	15.782	15.239	35.875					This study
ZK3607-530A	Pyrite	in mica schists	15.233	15.168	35.361					This study
average			15.884	15.245	35.934					

[a] Model ages (Million years) according to Stacey and Kramers (1975).

Dongshengmiao main orebody have been reported in our recent study (Gao et al., 2018). A majority of these samples are collected from drill cores, and the others are from underground mines.

Sulfide minerals were handpicked under a binocular microscope from hand-specimens. Separated sulfide minerals were then crushed and pulverized in an agate mortar, followed by digestion using a mixture of distilled HNO_3 and HCl. After incipient dryness, decomposed samples were redissolved in HBr. Pb was separated and purified by conventional ion-exchange chromatography on columns containing AG1-X8 exchange resin (Li et al., 2015). Pb isotope ratios were measured using a Multi-Collector ICP-MS (MC-ICP-MS; Nu Instruments) at the Laboratory of Isotope Geology, Ministry of Land and Resources of China (He et al., 2005). Samples were Tl-doped to facilitate corrections for instrumental mass bias based on an exponential dependence on mass law, largely similar to the procedure described by Belshawa et al. (1998) and Zhu et al. (2000). Repeat analyses of the NBS 981 Pb isotopic standard gave a reproducibility (2σ) of $^{208}Pb/^{206}Pb = 2.16736 \pm 0.00066$,

$^{207}Pb/^{206}Pb = 0.91488 \pm 0.00028$, $^{206}Pb/^{204}Pb = 16.9386 \pm 0.0131$, $^{207}Pb/^{204}Pb = 15.4968 \pm 0.0107$, and $^{208}Pb/^{204}Pb = 36.7119 \pm 0.0331$ at the 2SD level.

The concentrations of U, Th and Pb were measured for pyrite, chalcopyrite, sphalerite and pyrrhotite using inductively coupled plasma mass spectrometry (ICP-MS) performed at the National Research Center for Geoanalysis, China. Approximately 50 mg of sample powder was dissolved with HNO_3-HF at 190 °C in Teflon bombs for 24 h. After cooling, the Teflon vessels with the resulting solution were heated on a hotplate until dry. Subsequently, HNO_3 was added, and the sample was heated again until dry to drive out HF. Finally, the material was redissolved in 5 mL of HNO_3 (8 mol/L) and diluted to 50 mL with deionized water. The obtained solution was used for ICP-MS (TJA PQ-ExCell) analysis, with relative standard deviations for U, Th and Pb within 5% based on replicate measurements of standard samples.

5. Results

5.1. Pb isotope data

All Dongshengmiao sulfide Pb isotope data obtained in this study are shown in Table 1 and plotted in Fig. 6, together with those from Li et al. (1986), Ding and Jiang (2000) and Gao et al. (2018). The overall results of Pb isotope compositions show a wide range in $^{206}Pb/^{204}Pb$ (14.928–16.441), $^{207}Pb/^{204}Pb$ (15.045–15.338) and $^{208}Pb/^{204}Pb$ (34.975–36.637), comparable with those reported for Tanyaokou, 30 km to the west (Fig. 1A; Ding and Jiang, 2000).

In more detail, Pb isotope ratios of the massive sulfides comprising stratiform orebodies are characterized by a relative unradiogenic isotope composition ($^{206}Pb/^{204}Pb$ = 14.963–15.396; $^{207}Pb/^{204}Pb$ = 15.064–15.181; $^{208}Pb/^{204}Pb$ = 34.975–35.528). The results of Pb-Pb model ages calculated for massive sulfide samples using the two-stage model of Stacey and Kramers (1975) are ca. 1950 Ma–1750 Ma (Table 1), in agreement with the single zircon U-Pb age (ca. 1750 Ma; Li et al., 2007) and the whole rock Sm-Nd model age of the metabasalt rocks from the host sequence (t_{DM} = 1767–1867 Ma; Peng and Zhai, 1997).

In terms of mean Pb isotope compositions, our data suggest that basal stratiform Cu-S orebodies in the Shujigou and Zenglongchang Formations have less radiogenic Pb compositions than the other orebodies that occurred in the Agulugou Formation (Table 1). Chalcopyrite samples from the basal Cu-bearing quartzites have similar Pb isotope compositions as the ore sulfides from the adjacent 1# and 8# S orebodies (Table 1; Fig. 7). Pb isotope data for ore sulfides from the brecciated Zn-Pb ores collected from different positions of the main orebody vary marginally, with $^{206}Pb/^{204}Pb$ = 15.154–15.167, $^{207}Pb/^{204}Pb$ = 15.148–15.153 and $^{208}Pb/^{204}Pb$ = 35.300–35.326, which are similar to those of massive pyrites also from the main orebody ($^{206}Pb/^{204}Pb$ = 15.197–15.202; $^{207}Pb/^{204}Pb$ = 15.151–15.158; $^{208}Pb/^{204}Pb$ = 35.356–35.363).

By contrast, Pb isotope compositions of vein-type ores form a linear trend and show a wider range of values, with $^{206}Pb/^{204}Pb$ ranging from 15.187 to 17.540, $^{207}Pb/^{204}Pb$ ranging from 15.147 to 15.482, and $^{208}Pb/^{204}Pb$ ranging from 35.325 to 37.590 (Table 1; Fig. 6). Pb isotope data of disseminated pyrites cover a similar range to those of vein-type sulfides but extend towards even more radiogenic compositions (Table 1; Fig. 7). Pb isotopic data of disseminated pyrites and vein-type ores form a single line with a slope of 0.1427 (r^2 = 0.9634) on the diagram of $^{207}Pb/^{204}Pb$ vs. $^{206}Pb/^{204}Pb$ (Fig. 6).

5.2. Contents of U, Th and Pb in sulfides

The results (Table 1) showed that the Dongshengmiao sulfides (sphalerite, pyrrhotite, pyrite and chalcopyrite) have high-Pb but low-U content (< 0.51 ppm). Very low U/Pb (< 0.001, with one exception of 0.02) and Th/Pb (< 0.003, with one exception of 0.01) ratios indicate that the addition of radiogenic Pb after the formation of these sulfides is negligible, and no age correction is needed.

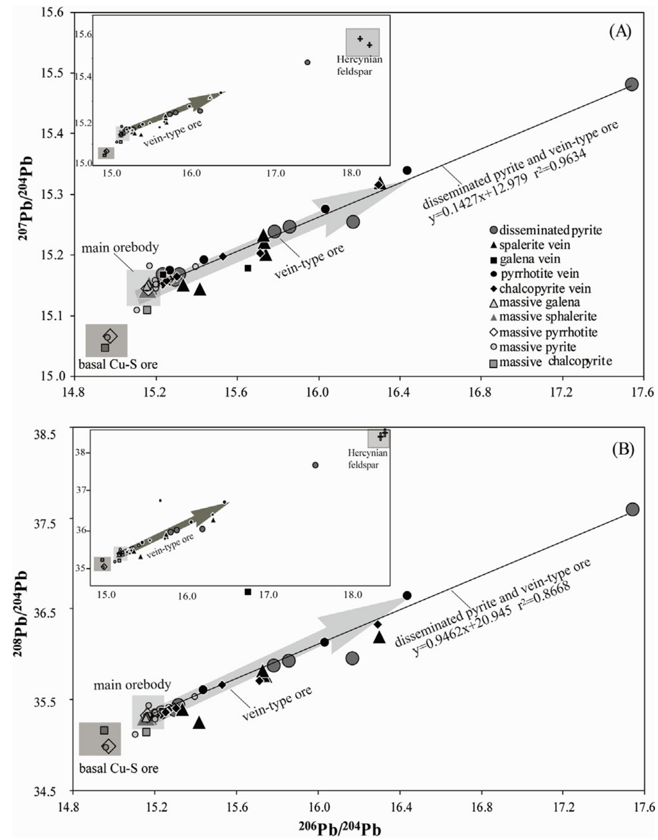

Fig. 6. Pb isotope compositions of various sulfides from the Dongshengmiao deposit. Data of sulfides are from Table 1 and data of Hercynian feldspars are from Zhu et al. (2006). Disseminated pyrites were collected from mica schists in the lower part of the Agulugou Formation; sphalerite vein, galena vein, pyrrhotite vein and chalcopyrite vein refer to sphalerite, galena, pyrrhotite and chalcopyrite collected from vein-type ores in the orebodies of 9#～11# or mica schists; massive galena, massive sphalerite, massive pyrrhotite, massive pyrite and massive chalcopyrite refer to galena, sphalerite, pyrrhotite, pyrite and chalcopyrite collected from stratiform orebodies (1#, 2#, 4#, 5#, and 8# and basal Cu orebody). Note that the Pb isotope compositions of vein-type ores in carbonaceous mica schist are more radiogenic and more scattered relative to massive ore sulfides from stratiform orebodies in both the $^{207}Pb/^{204}Pb$ vs. $^{206}Pb/^{204}Pb$ plot (A) and the $^{208}Pb/^{204}Pb$ vs. $^{206}Pb/^{204}Pb$ plot (B).

6. Discussion

6.1. Genetic relationship between the stratiform Cu-Zn-Pb and S orebodies

The effectiveness of the Pb isotope system in unraveling multistage sulfide mineralization events (Brevart et al., 1982; Paiement et al., 2012) and determining different metal sources (Romer and Wright, 1993; Kinnaird et al., 2002; Beaudoin, 1997; Haest et al., 2010) was demonstrated by early researchers in the studies of some large polymetallic metallogenic systems. Stratiform S orebodies are widely regarded as being of syngenetic origin, whereas the metallogenic processes of the most economical Cu-Zn-Pb ore, as well as its possible genetic links to the syngenetic S ore of the Proterozoic age, still remain controversial. A large-scale remobilization has been proposed to account for the formation of the Dongshengmiao Cu-Zn-Pb orebodies by some recent studies (Zhang et al., 2010; Zhong et al., 2015a; Zhong and Li, 2016). In this model, the parental sulfides have almost been totally redistributed during regional metamorphism and deformation;

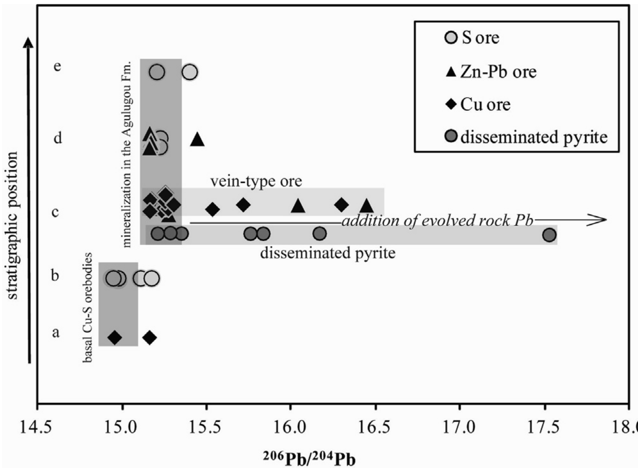

Fig. 7. Pb isotope compositions of sulfides from different ore horizons of the Dongshengmiao deposit. Data are from Table 1. a, basal Cu ore (Shujigou Formation); b, lower S orebodies (1# and 8#; Zenglongchang Formation); c, strata-bound Cu-Zn-Pb orebodies (9#～11#) hosted by carbonaceous mica schists (lower part of the Agulugou Formation), which contain pervasive disseminated pyrites; d, Dongshengmiao main orebody (2#); e, upper S orebodies (3#～5#; upper part of the Agulugou Formation). Note that Pb isotope data of disseminated pyrites cover a similar range to those of vein-type ores but extend towards even more radiogenic compositions.

therefore, whether different ore types at Dongshengmiao were originally formed during a single continuous metallogenic process still remains ambiguous.

As shown in Table 1 and Fig. 7, the analyses of various sulfides from the brecciated Cu-Zn-Pb ores are tightly clustered ($^{206}Pb/^{204}Pb$ = 15.154–15.167) and similar to those of the syngenetic massive pyrites ($^{206}Pb/^{204}Pb$ = 15.197–15.202) from the same stratigraphic position (Dongshengmiao main orebody), which are characterized by a very unradiogenic isotope composition and a Paleoproterozoic Pb-Pb model age. Furthermore, basal chalcopyrite samples collected from the Shujigou Formation have similar Pb isotope compositions to the massive ore sulfides from the adjacent stratiform S orebodies in the Zenglongchang Formation (Table 1; Fig. 6). These characteristics rule out any possibility that extraneous metals from younger hydrothermal fluids associated with either Permian orogeny or Cretaceous orogeny (Peng et al., 2007a; Zhong and Li, 2016) were involved in the formation of brecciated or massive Cu-Zn-Pb ores. In addition, the great similarity of the S isotope composition of Cu-Zn-Pb ores and syngenetic S ores (Gao et al., 2015) also indicates a single continuous metallogenic process. Otherwise, these Cu-Zn-Pb ores would have different isotope compositions with syngenetic S ores from the same stratigraphic position because of the mobilization at different periods and/or derivation from different sources.

As noted above, massive sulfide orebodies at Dongshengmiao can be divided into two sub-groups on the basis of their stratigraphic horizons, ore types and vertical metal zoning (Fig. 2; Xia, 1992; Jiang, 1994). Accordingly, basal Cu-S ores have less radiogenic Pb compositions than the other sulfide ores that occurred in the Agulugou Formation (Fig. 7). This shift may be related to Pb radiogenic growth in the underlying basement, or the upper Agulugou stratabound mineralization may have interacted with increasing crustal Pb, characterized by elevated $^{206}Pb/^{204}Pb$ values, during the formation of the Dongshengmiao deposit. Some evidence suggests the former. On the one hand, obvious epigenetic features of Cu-Zn-Pb ores in the Agulugou Formation indicate that these base metal ores may represent a discrete influx of ore fluid separated in time from basal stratiform Cu-S orebodies in the Shujigou and Zenglongchang Formations; on the other hand, no systematic change in Pb isotope ratios with stratigraphic position is observed in multiple ore horizons in the Agulugou Formation (Fig. 7), likely indicating a very minor involvement of rock Pb during the formation of stratiform orebodies. The very minor involvement of upper-crustal material during formation of the deposit was also responsible for the exceedingly unradiogenic Pb signature.

6.2. Constraints on the origin of vein-type ores

Notwithstanding their lower grades, vein-type sulfide ores still constitute an important ore (especially Cu ore) resource in the Dongshengmiao deposit. Therefore, it is important to investigate the genetic relationship between the vein-type ores and stratiform orebody in order to establish the deposit's metallogenesis. Although Pb isotope compositions of vein-type ores are more radiogenic and more scattered relative to those of massive ore sulfides both in the $^{208}Pb/^{204}Pb$ vs. $^{206}Pb/^{204}Pb$ and the $^{207}Pb/^{204}Pb$ vs. $^{206}Pb/^{204}Pb$ diagrams (Fig. 6), the less radiogenic end member of these vein-type ores projects towards the Pb isotope composition of the overlying Dongshengmiao main orebody (Fig. 6). Approximately half of the vein-type Cu-rich ores have similar Pb isotope compositions to the overlying Proterozoic syngenetic ores (Fig. 7). It is thus possible that these unradiogenic sulfide veins originally contained Pb isotope compositions that resembled those from the overlying stratiform orebodies. Notably, the linear trend shown by vein-type ores suggests that they may include an extraneous contribution of lead in addition to a lead source common to stratiform orebodies.

Based mainly on the results from decrepitating fluid inclusions, Peng et al. (2007a) suggested that Hercynian granitic magmatic fluids overprinted the Proterozoic exhalative mineralization. Although the Hercynian granitoids at Dongshengmiao are volumetrically large, there is no robust evidence in support of a significant input of metals (Xia, 1992; Jiang, 1993). The most reliable initial Pb isotope compositions of the Hercynian granitoids in the Langshan district were obtained from the feldspar minerals (Zhu et al., 2006) because these minerals normally have the lowest U/Pb and Th/Pb ratios and relatively little radiogenic Pb has been incorporated over time from ^{238}U, ^{235}U, and ^{232}Th decay (e.g., Gancarz and Wasserburg, 1977; Kamber and Moorbath, 1998). However, Pb isotope ratios of the bulk of the sulfide ores at Dongshengmiao (all massive and approximately half of sulfide veins) are characterized by an unradiogenic isotope composition and a Paleoproterozoic Pb-Pb model age, which are significantly different than those of the Hercynian feldspars in the Langshan district ($^{206}Pb/^{204}Pb$ = 18.179–18.303; Zhu et al., 2006). Thus, Pb isotope signatures of these Hercynian feldspars would be too high to explain the radiogenic Pb admixed in the vein-type ores observed in this study (Fig. 6). The lack of intermediate Pb isotope values (a significant Pb isotope gap) between the Hercynian feldspars and the vein-type ores (Fig. 6) is also evidence that the radiogenic signature of these veins does not represent Hercynian granitic overprinting. On the other hand, even if their radiogenic end-member was represented by the radiogenic Pb derived from the Hercynian magmatism, a very minor proportion (～10%) of the Hercynian granitic input in the formation of the vein-type sulfide ores can be estimated by their means (Table 1). In addition, early Permian granitoids widely occurred in the northwest of the Dongshengmiao deposit and have no obvious spatial relationship with Cu ores, which mainly occurred as a cystic-shaped breccias zone and associated sulfide veins in the Agulugou Formation, together with the basal stratiform Cu orebody (Jiang, 1993). The chemical and H-O isotope compositions of ore-fluids during Cu-Zn-Pb mineralization did not have characteristics of magmatic hydrothermal fluids (Miu and Ran, 1992; Zhong and Li, 2016). Our recent Fe and S isotope studies (Gao et al., 2015, 2016) also indicated that vein-type ores and associated disseminated pyrites in mica schist were unlikely to have a significant granitic input. Consequently, these characteristics suggest that addition of radiogenic Pb during Hercynian magmatism to account for the highly radiogenic nature of the vein-type ores is deemed unlikely.

Although Dongshengmiao has been subjected to only relatively low-grade metamorphism (lower greenschist facies; Zhong et al., 2015a), previous studies suggested that the Dongshengmiao deposit experienced metamorphic temperatures in the range of 250–450 °C (Miu and Ran, 1992) and penetrative ductile deformation (Zhong et al., 2015a). It would not be unreasonable to think that mobilized host rock lead contributed to vein-type ores during regional metamorphism as inferred by Ding and Jiang (2000). As noted above, carbonaceous mica schist hosts vein-type ores, as well as pervasive disseminated pyrites. In this study, the highly radiogenic nature of disseminated pyrite in carbonaceous mica schist can easily be explained by the addition of evolved rock lead during metamorphic crystallization. Noteworthy Pb isotopic overlap exists between vein-type ores and disseminated pyrites (Fig. 6; Fig. 7), suggesting that the radiogenic lead in sulfide veins was most likely derived from surrounding host rocks rather than external metal sources.

In terms of Pb isotope compositions relative to massive or brecciated ores, the vein-type Cu-rich ores and disseminated pyrites are more susceptible to the effect of Pb from their host-rocks during greenschist face metamorphisms. Thus, different ore types in the Dongshengmiao deposit have been affected by variable degrees of metamorphic recrystallization and local mobilization. As noted above, the low U/Pb and Th/Pb ratios of the Dongshengmiao sulfides imply that the radiogenic Pb growth from U and Th decay after the formation of these sulfides is negligible. Therefore, the scatter of Pb isotope compositions of the Dongshengmiao Cu-Zn-Pb ores shows that lead was not homogenized regionally during subsequent metamorphism, which seems not to be supportive of a deposit-scale remobilization. It seems plausible that mobilized host rock lead had contributed to a portion of the vein-type ores and disseminated pyrites during a local and small-scale remobilization. Therefore, significant amounts of metals from younger fluids, inferred to have overprinted the Proterozoic mineralization during a large-scale remobilization (Zhong and Li, 2016), is unlikely.

6.3. A Genetic model

6.3.1. Age of stratiform sulfide orebodies

As noted above, Pb isotope ratios of various massive ore sulfides from stratiform orebodies are characterized by a relative unradiogenic isotope composition ($^{206}Pb/^{204}Pb$ = 14.963–15.396). The results of Pb-Pb model ages calculated for massive sulfide samples using the two-stage model of Stacey and Kramers (1975) are from ca. 1950 Ma to 1750 Ma (Table 1), in agreement with the single zircon U-Pb age (ca. 1750 Ma; Li et al., 2007) and the whole rock Sm-Nd model age of the metabasalt from the host rocks (t_{DM} = 1767–1867 Ma; Peng and Zhai, 1997). Combining U-Pb zircon, detrital ziron, Sm-Nd model and fossil ages (Bai, 1993; Li et al., 2007; Peng and Zhai, 1997; Gong et al., 2016), we may conclude that the bulk of the sulfide mineralization at Dongshengmiao occurred at the late Paleoproterozoic.

Obviously, younger fluids with normal crustal Pb abundance in Phanerozoic time (Leach et al., 1998) also unlikely played an important role in the Cu-Zn-Pb endowment at Dongshengmiao. Consequently, significant amounts of Pb (and therefore likely S and other metals) from younger fluids, inferred to have overprinted the Proterozoic mineralization during either Permian orogeny or Cretaceous orogeny (Peng et al., 2007a; Zhong and Li, 2016), is not favored.

6.3.2. Metallogenic process

Pb isotope ratios of the massive sulfides comprising multiple ore horizons are characterized by a relative unradiogenic isotope composition. Importantly, the substantial similarity of the Pb isotope composition between the stratiform Cu-Zn-Pb and S orebodies suggests that the bulk of the Cu-Zn-Pb ores belong to the same polymetallic metallogenic system with the syngenetic S ores of the Proterozoic age.

As noted above, stratiform orebodies at Dongshengmiao can be divided into two sub-groups on the basis of their stratigraphic horizons, ore types and vertical metal zoning (Fig. 2; Xia, 1992; Jiang, 1994). Accordingly, basal stratiform Cu-S orebodies in the Shujigou and Zenglongchang Formations have less radiogenic Pb compositions than the other sulfide orebodies that occurred in the upper Agulugou Formation (Fig. 6; Fig. 7), which is related to either Pb radiogenic growth in the source rocks or the growing introduction of host rock Pb during formation of the Dongshengmiao deposit. Our Pb isotope data lean towards the former scenario, namely, that two main mineralization events in the Proterozoic were likely involved in the formation of the Dongshengmiao deposit because no systematic change in Pb isotope ratios with stratigraphic position is observed in multiple ore horizons in the Agulugou Formation (Fig. 7). Basal Cu-S ores, which formed during the early mineralization event, present the Pb isotope compositions of the original ore-bearing fluid in the Dongshengmiao SEDEX mineralizing system. By contrast, different ore types in the Agulugou Formation were largely formed during a single continuous metallogenic process. In the vertical direction, metal abundance in this formation varies from Cu to Zn-Pb to Fe (pyrite, pyrrhotite and siderite) from bottom to top. Mineralization in the Agulugou Formation is associated with multiple adjacent orebodies and may represent a discrete influx of ore fluid separated in time from basal Cu-S ores by a considerable interval to allow for deposition of ~500 m carbonaceous shale.

The above processes are consistent with the conventional SEDEX model involving focused circulations of hydrothermal fluids, which could form various ore styles during a long-term metallogenic event. Different ore types have been affected by variable degrees of metamorphic recrystallization and local mobilization, whereas the Dongshengmiao mineralizing system has unlikely been affected by a significant input from, or overprinting by, younger fluids. A small part of the sulfide veins and disseminated pyrites experienced a minor addition of evolved rock lead during greenschist face metamorphisms. Meanwhile, the radiogenic sulfide veins and associated disseminated pyrites in this study constitute a very minor ore resource at Dongshengmiao. Therefore, the significant introduction of external metals from younger fluids inferred by earlier researchers (Peng et al., 2007a; Zhong and Li, 2016) remains to be clarified by future studies.

7. Conclusions

The substantial similarity of the Pb isotope compositions between the main types of Cu-Zn-Pb ores and massive S orebodies suggests that the bulk of the Cu-Zn-Pb ores at Dongshengmiao belong to the same polymetallic metallogenic system with the syngenetic S ores of the Proterozoic age, whereas noteworthy Pb isotope overlap exists between the vein-type ores and associated disseminated pyrites suggests that the radiogenic lead in sulfide veins was most likely derived from surrounding host rocks rather than external metal sources.

Acknowledgments

This research was financially supported by the CAGS Research Fund (No. YYWF201603). The authors would like to thank Zhihong Li, Jin Li and Shizhen Li for their meticulous guidance during the chemical and instrumental experiments at CAGS. Comments by the Editor-in-Chief Guochun Zhao, the Associate Editor Xianhua Li, Prof. Åke Johansson, Prof. Ryan Mathur and an anonymous reviewer have improved the manuscript significantly.

Appendix A. Supplementary data

Supplementary data to this article can be found online at https://doi.org/10.1016/j.precamres.2018.09.002.

References

Anderson, B.R., Gemmell, J.B., Nelson, D.R., 2002. Lead isotope evolution of mineral deposits in the Proterozoic Throssell Group, Western Australia. Econ. Geol. 97 (4),

897–911. https://doi.org/10.2113/gsecongeo.97.4.897.
Ayuso, R.A., Till, A.B., Slack, J.F., Forni, F., 2014. Pb isotope geochemistry of stratabound Zn-Pb(-Ag-Au-Ba-F) deposits and occurrences in the Nome Complex, Seward Peninsula, Alaska: Metal sources and regional comparisons. In: Dumoulin, J.A., Till, A.B. (Eds.), Reconstruction of a Late Proterozoic to Devonian continental margin sequence, Northern Alaska, its paleogeographic significance, and contained base-metal sulfide deposits. Geological Society of America Special Paper 506, 213–234, doi:10.1130/2014.2506(07).
Bai, J., 1993. The Precambrian geology and Pb-Zn mineralization in the Northern margin of North China Platform. Geological Publishing House, Beijing (in Chinese with English abstract).
Bao, C., Chen, Y.L., Zhu, X.K., Zhao, J.X., 2018. Attribution of the Langshan Tectonic Belt: evidence from zircon U-Pb ages and Hf isotope compositions. Geosci. Front. https://doi.org/10.1016/j.gsf.2018.03.001.
Beaudoin, G., 1997. Proterozoic Pb isotope evolution in the Belt-Purcell Basin: Constraints from syngenetic and epigenetic sulfide deposits. Econ. Geol. 92, 343–350. https://doi.org/10.2113/gsecongeo.92.3.343.
Belshaw, N.S., Freedman, P.A., O'Nions, R.K., 1998. A new variable dispersion double-focusing plasma mass spectrometer with performance illustrated for Pb isotopes. Int. J. Mass Spectrom. 181, 51–58. https://doi.org/10.1016/S1387-3806(98), 14150-7.
Brevart, O., Dupre, B., Allegre, C.J., 1982. Metallogenic provinces and the remobilization process studied by lead isotopes: Lead-zinc ore deposits from the southern Massif Central, France. Econ. Geol. Bull. Soc. Econ. Geol. 77, 564–575. https://doi.org/10.2113/gsecongeo.77.3.564.
Ding, T.P., Jiang, S.Y., 2000. Stable isotope study of the Langshan polymetallic mineral district, Inner Mongolia, China. Res. Geol. 50, 25–38. https://doi.org/10.1111/j.1751-3928.2000.tb00053.x.
Gancarz, A.J., Wasserburg, G.J., 1977. Initial Pb of the Amîtsoq gneiss, West Greenland, and implications for the age of the Earth. Geochim. Cosmochim. Acta 41 (9), 1283–1301. https://doi.org/10.1016/0016-7037(77), 90073-4.
Gao, Z.F., Zhu, X.K., Luo, Z.H., Sun, J., Zhang, F.F., Gao, W.G., Wang, B.L., Zhong, C.H., 2014. Geologic and geochemical characteristics of the main ore-bearing rock series in Dongshengmiao super-large polymetallic sulfide deposit and the indication significance of ore genesis. Acta Petrol. et Miner. 33 (5), 825–840 (in Chinese with English abstract).
Gao, Z.F., Zhu, X.K., Zhang, K., Luo, Z.H., Bao, C., Tang, C., 2015. Sulfur source and mineralization process of the Dongshengmiao polymetallic sulfide deposit in the Langshan ore belt, Inner Mongolia. Acta Petrol. Sin. 31 (12), 3725–3731 (in Chinese with English abstract).
Gao, Z.F., Zhu, X.K., Gao, W.G., Wang, B.L., Sun, J., Luo, Z.H., Bao, C., Tang, C., 2016. Fe isotopic characteristics of the Dongshengmiao and Tanyaokou polymetallic sulfide deposits in Inner Mongolia and their metallogenic significance. Acta Geol. Sin. 90, 352–360 (in Chinese with English abstract).
Gao, Z.F., Zhu, X.K., Sun, J., Luo, Z.H., Bao, C., Tang, C., Ma, J.X., 2018. Spatial evolution of Zn-Fe-Pb isotopes of sphalerite within a single orebody: a case study from the Dongshengmiao ore deposit, Inner Mongolia. China. Miner. Deposita. 53, 55–65. https://doi.org/10.1007/s00126-017-0724-x.
Gong, W.B., Hu, J.M., Li, Z.H., Dong, X.P., Liu, Y., Liu, S.C., 2016. Detrital zircon U-Pb dating of Zhaertai Group in the North Margin Rift Zone of North China Craton and its implications. Acta Petrol. Sin. 32 (7), 2151–2165 (in Chinese with English abstract).
Haest, M., Schneider, J., Cloquet, C., 2010. Pb isotopic constraints on the formation of the Dikulushi Cu-Pb-Zn-Ag mineralisation, Kundelungu Plateau (Democratic Republic of Congo). Miner. Deposita 45 (4), 393–410. https://doi.org/10.1007/s00126-010-0279-6.
He, X.X., Zhu, X.K., Yang, C., Tang, S.H., 2005. High-precision analysis of Pb isotope ratios using MC-ICP-MS. Acta Geosci. Sinica 26 (Sup.), 19–22 (in Chinese with English abstract).
Hu, C.S., Li, W.B., Xu, C., Zhong, R.C., Zhu, F., Qiao, X.Y., 2015. Geochemistry and petrogenesis of Permian granitoids in the Northwestern margin of the North China Craton: insights from the Dongshengmiao pluton, Inner Mongolia. Int. Geol. Rev. 57 (14), 1843–1860.
Jiang, X.Q., 1993. Geological characteristics of the Dongshengmiao pyrite-polymetallic sulfide deposit, Inner Mongolia. China Academic Journal Electronic Publishing House 27, 103–115 (in Chinese with English abstract).
Jiang, X.Q., 1994. Evidence for contemporaneous faults in the Dongshengmiao sulfide polymetallic ore district in Inner Mongolia and the genesis of the ore deposit. Miner. Deposits 13, 49–60 (in Chinese with English abstract).
Kamber, B.S., Moorbath, S., 1998. Initial Pb of the amitsoq gneiss revisited: implication for the timing of early Archaean crustal evolution in West Greenland. Chem. Geol. 150 (1–2), 19–41. https://doi.org/10.1016/S0009-2541(98)00059-X.
Kinnaird, J.A., Ixer, R.A., Barreiro, B., Nex, P.A.M., 2002. Contrasting sources for lead in Cu-polymetallic and Zn-Pb mineralization in Ireland: constraints from lead isotopes. Miner. Deposita 27, 495–511. https://doi.org/10.1007/s00126-001-0252-5.
Leach, D.L., Hofstra, A.H., Church, S.E., Snee, L.W., Vaughn, R.B., Zartman, R.E., 1998. Evidence for Proterozoic and Late Cretaceous-Early Tertiary ore-forming events in the Coeur d'Alene district, Idaho and Montana. Econ. Geol. 93, 347–359. https://doi.org/10.2113/gsecongeo.93.7.1106.
Li, Q.L., Chen, F.K., Guo, J.H., Li, X.H., Yang, Y.H., Siebel, W., 2007. Zircon ages and Nd-Hf isotopic composition of the Zhaertai Group (Inner Mongolia): evidence for early Proterozoic evolution of the northern North China Craton. J. Asian Earth Sci. 30, 573–590.
Li, S.Z., Ma, J.X., Zhu, X.K., Tang, S.H., 2015. Pb isotopic fractionation during the ion exchange process and the modification of purification methods for isotope determination by MC-ICP-MS. Acta Petrol. et Miner. 34 (5), 785–792 (in Chinese with English abstract).
Li, Z.L., Xu, W.D., Pang, W.Z., 1986. S, Pb, C and O isotopic compositions and ore genesis of the stratabound polymetallic sulfide deposits in middle Inner Mongolia, China. Geochem 1, 13–22 (in Chinese with English abstract).
Liu, Y., 2012. Geochemical and Chronological Characteristics of the Granitic Gneisses and Intrusive Rocks from Dongshengmiao Region, Inner Mongolia and their Tectonic Implications. Doctoral dissertation. Lanzhou University (in Chinese with English abstract).
Long, L.Z., 2009. Geological Characteristics and Genesis Analysis of the Dongshengmiao Lead-zinc Ore Deposit in the Inner Mongolia. Dissertation. Central South University (in Chinese with English abstract).
Marcoux, E., 1998. Lead isotope systematics of the giant massive sulphide deposits in the Iberian Pyrite Belt. Miner. Deposita 33, 45–58. https://doi.org/10.1007/s001260050132.
Miu, Y.X., Ran, C.Y., 1992. Geological and geochemical characteristics of the Dongshengmiao Pb-Zn-S deposit of submarine exhalative origin, Inner Mongolia. Geochimica 4, 375–382 (in Chinese with English abstract).
Mukasa, S.B., Vidal, C.E., Injoque-Espinoza, J., 1990. Pb isotope bearing on the metallogenesis of sulfide ore deposits in central and southern Peru. Econ. Geol. 85, 1438–1446. https://doi.org/10.2113/gsecongeo.85.7.1438.
Paiement, J.P., Beaudoin, G., Paradis, S., Ullrich, T., 2012. Geochemistry and metallogeny of Ag-Pb-Zn veins in the Purcell Basin, British Columbia. Econ. Geol. 107, 1303–1320. https://doi.org/10.2113/econgeo.107.6.1303.
Peng, R.M., Zhai, Y.S., 1997. The confirmation of the metamorphic double-peaking volcanic rocks in Langshan Group of the Dongshengmiao ore district, Inner Mongolia and its significance. Earth Sci. J. China Univ. Geosci. 22, 589–594 (in Chinese with English abstract).
Peng, R.M., Zhai, Y.S., 2004. The characteristics of hydrothermal exhalative mineralization of the Langshan-Zhaertai belt, Inner Mongolia. China Earth Science Front. 11, 257–268 (in Chinese with English abstract).
Peng, R.M., Zhai, Y.S., Han, X.F., Wang, J.P., Wang, Z.G., Qin, J.W., 2007a. Magmatic hydrothermal overprinting in the Mesoproterozoic Dongshengmiao deposit, Inner Mongolia: geological and fluid inclusion evidences. Acta Petrol. Sin. 23, 145–152.
Peng, R.M., Zhai, Y.S., Han, X.F., Wang, Z.G., Wang, J.P., Shen, C.L., Chen, X.F., 2007b. Mineralization response to the structural evolution in the Langshan orogenic belt, Inner Mongolia. Acta Petrol. Sin. 23, 679–688 (in Chinese with English abstract).
Peng, R.M., Zhai, Y.S., Han, X.F., Wang, Z.G., Wang, J.P., Liu, J.J., 2007c. Synsedimentary volcanic activities in the cracking process of the Mesoproterozoic aulacogen of passive continental margin in the Langshan-Zhaertai area, Inner Mongolia, and its indicating significance. Acta Petrol. Sin. 23 (5), 1007–1017.
Peng, R.M., Zhai, Y.S., Wang, Z.G., 2000. Ore-controlling synchronous faults of Mesoproterozoic Dongshengmiao and Jiashengpan SEDEX-type ore deposits, Inner Mongolia. Earth Science. J. China Univ. Geosci. 4, 404–410 (in Chinese with English abstract).
Potra, A., Macfarlane, A.W., 2014. Lead isotope studies of the Guerrero composite terrane, west-central Mexico: implications for ore genesis. Miner. Deposita 49, 101–117. https://doi.org/10.1007/s00126-013-0477-0.
Romer, R.L., Wright, J.E., 1993. Lead mobilization during tectonic reactivation of the western Baltic Shield. Geochim. Cosmochim. Acta 57, 2555–2570. https://doi.org/10.1016/0016-7037(93)90417-U.
Rui, Z.Y., Shi, L.D., Fang, R.H., 1994. Geology of Nonferrous Metallic Deposits in the Northern Margin of the North China Landmass and its Adjacent Area. Geological Publishing House, Beijing (in Chinese with English abstract).
Stacey, J.S., Kramers, J.D., 1975. Approximation of terrestrial lead isotope evolution by a two-stage model. Earth Planet. Sci. Lett. 26, 207–221. https://doi.org/10.1016/0012-821X(75)90088-6.
Velasco, F., Pesquera, A., Herrero, J.M., 1996. Lead isotope study of Zn-Pb ore deposits associated with the Basque-Cantabrian basin and Paleozoic basement, northern Spain. Miner. Deposita 31, 84–92 10.1007 /BF00225398.
Wu, Y.F., Zeng, J.N., Cao, J.J., Wu, Z.Q., Chen, J.H., Zhou, S.D., Lu, S.F., Li, X.F., 2013. Zircon U-Pb ages and Hf isotopes of Hercynian intrusion in Dongshengmiao, Inner Mongolia. Geol. Sci. Technol. Inform. 32, 22–30 (in Chinese with English abstract).
Xia, X.H., 1992. Ore-forming characteristics and genetic discussion of the Dongshengmiao polymetallic pyrite deposits in Langshan metallogenic belt, Inner Mongolia. Miner. Deposit. 11, 374–383 (in Chinese with English abstract).
Xia, X.H., Zhao, X., 1990. Origin of brecciated-type ores of the Dongshengmiao polymetallic sulfide deposit, Inner Mongolia. Geol. Prospect. 26 (7), 30–41 (in Chinese with English abstract).
Xiu, S.Y., 1987. Origin of the Tanyaokou-Dongshengmiao polymetallic sulfide deposits. Geol. Chem. Miner. 02, 1–12 (in Chinese).
Zhai, Y.S., Peng, R.M., Chen, C.X., Cai, K.Q., Deng, J., Chen, X.M., Cheng, X.J., Wang, J.P., 2008. Genesis and Structure of Major Metallogenic Series of China. Geological Publishing House, Beijing (in Chinese with English abstract).
Zhang, C., 2004. Hot-tectonic events and evolution of north margin of the North China Craton in Meso-Neoptoterozoic. Acta Scientiarum Naturalium Universitatis Pekinensis 40 (2), 232–240 (in Chinese with English abstract).
Zhang, Z.B., Li, J.H., Huang, C.Y., Liu, H., Zhao, Y.H., 2010. Study on genesis and ore prospecting of Dongshengmiao deposit in Inner Mongolia. J. Jilin Univ. (Earth Sci. Ed.) 40, 791–800 (in Chinese with English abstract).
Zhong, R.C., Li, W.B., 2016. The multistage genesis of the giant Dongshengmiao Zn-Pb-Cu deposit in western Inner Mongolia, China: syngenetic stratabound mineralization and metamorphic remobilization. Geosci. Front. 7 (3), 529–542.
Zhong, R.C., Li, W.B., Chen, Y.J., Ji, J.Q., Yang, Y.F., Hu, C.S., 2015a. Significant Zn-Pb-Cu remobilization of a syngenetic stratabound deposit during regional metamorphism: a case study in the giant Dongshengmiao deposit, northern China. Ore Geol. Rev. 64, 89–102.
Zhong, R.C., Li, W.B., Huo, H.L., 2015b. $^{39}Ar/^{40}Ar$ geochronological study on the Huogeqi Cu-Pb-Zn deposit in Inner Mongolia: a case of Proterozoic pre-enrichment followed

by Indosinian metamorphogenic mineralization. Acta Petrol. Sin. 31 (6), 1735–1748 (in Chinese with English abstract).
Zhou, C.X., Zhang, Y.G., Tang, P.Z., Chen, Y.M., Wang, S.L., Qi, Y.H., Yang, Q., 2012. A discussion on genesis and ore prospecting of Dongshengmiao deposit, Inner Mongolia. J. Jilin Univ. (Earth Sci. Ed.) 42, 1656–1664 (in Chinese with English abstract).
Zhu, X.K., O'Nions, R.K., Guo, Y., Belshaw, N.S., Rickard, D., 2000. Determination of natural Cu isotope variation by plasmas source mass spectrometry: Implications for use as geochemical tracers. Chem. Geol. 163, 139–149. https://doi.org/10.1016/S0009-2541(99)00076-5.
Zhu, X.Q., Zhang, Q., He, Y.L., Zhu, C.H., 2006. Lead isotopic composition and lead source of the Huogeqi Cu-Pb-Zn deposit, Inner Mongolia. China. Acta Geol. Sin. 80 (4), 528–539. https://doi.org/10.3321/j.issn:1000-9515.2006.04.009.